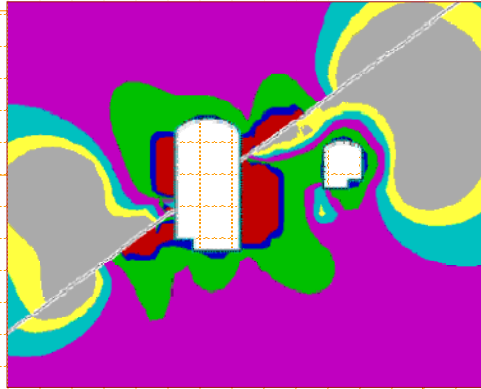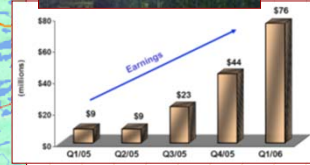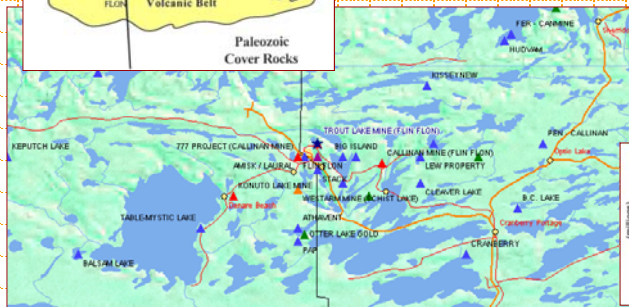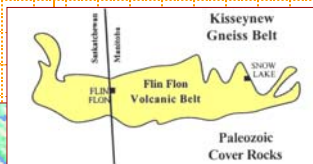EOSC433:

Geotechnical Engineering
Practice & Design

Lecture 8:
Stress Analysis
around Underground
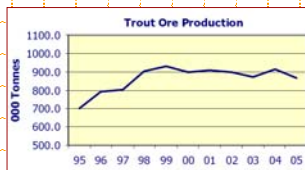Openings

Flin Flon Mining Belt

Since 1927, more than 29 mines have
been developed in the Flin Flon Greenstone
belt in the Canadian Shield, with
continuous production of zinc, copper,
silver, and gold since 1930.

1

Case History: Trout Lake Mine

	Tonnes	Au (g/t)	Ag (g/t)	Cu (%)	Zn (%)
Trout Lake					
Proven	1,433,000	1.0	11.1	1.4	4.7
Probable	1,058,000	1.7	20.5	2.5	4.0

The Trout Lake Cu-Zn sulphide deposit was discovered in 1976, with mining beginning in 1982. The deposit is a VMS-type deposit that involves two ore zones 500 m apart, which reach depths exceeding 1200 m.
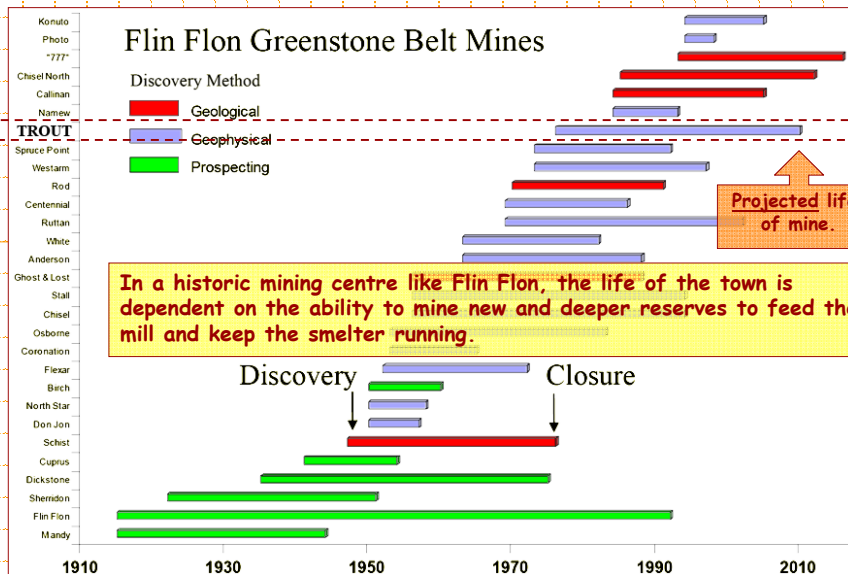
Flin Flon Mining Belt

Flin Flon Greenstone Belt Mines

Discovery Method
- Geological
- Geophysical
- Prospecting

Projected life of mine.

In a historic mining centre like Flin Flon, the life of the town is dependent on the ability to mine new and deeper reserves to feed the mill and keep the smelter running.
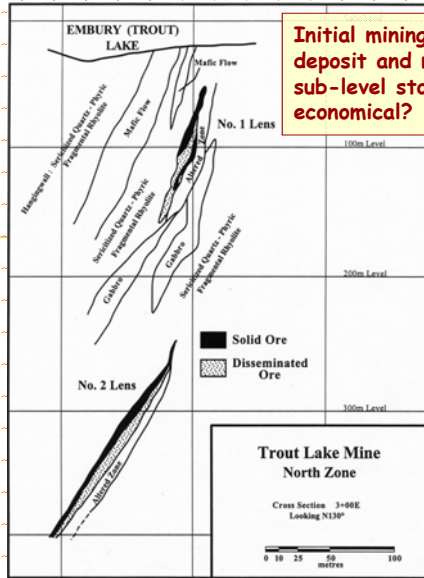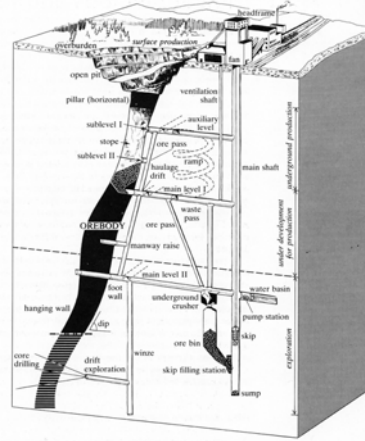
Discovery   Closure

Case History: Trout Lake Mine

Initial mining was carried out by ramping down to the deposit and mining it at relatively shallow depths through sub-level stoping. To what depths, though, will mining be economical?
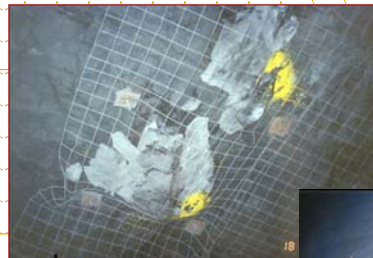
Brady & Brown (2006)

Case History: Trout Lake Mine
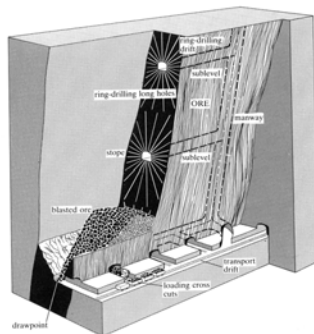
Trouble: Ground control, dilution and pillar stability problems encountered at 400m depth.

Case History: Trout Lake Mine

Eberhardt et al. (1997)

Ground control, dilution and drift stability problems encountered at 400m depth.
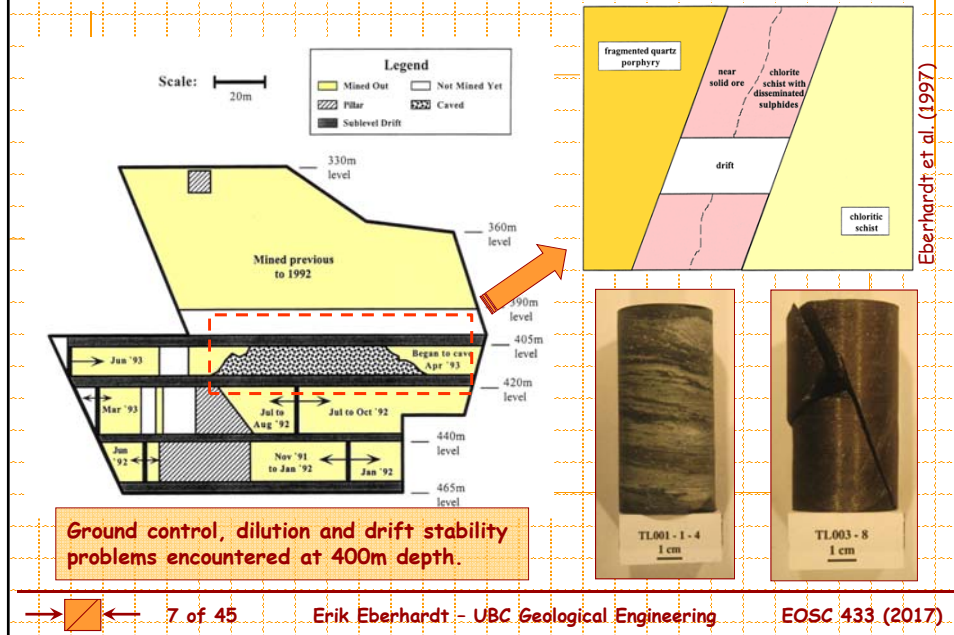
Case History: Trout Lake Mine Sill Pillar

First, stress-induced failure occurs in the weaker disseminated ore.

Then as failure evolves leaving solid ore unconfined, large blocks release and fall.

Eberhardt et al. (1997)

4

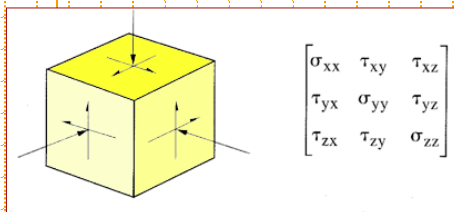# Case History: Trout Lake Mine

In 1990, a new zone of zinc-copper-silver-gold mineralization was discovered below the current workings. One underground drill hole intersected 105.9 m of 1.2 g/t gold, 17.8 g/t silver, 2.72% copper and 11.6% zinc?

If sill pillar stability is a problem at shallower depths, what will happen when the mine expands and goes deeper?

Stress-Controlled Instability Mechanisms

Structurally-controlled instabilities are generally driven by gravity (i.e., unidirectional force). Stress-controlled instabilities, however, are not activated by a single force, but by a tensor with six independent components. Hence, the manifestations of stress-controlled instability are more variable and complex than those of structurally-controlled failures.

$$\begin{bmatrix} \sigma_{xx} & \tau_{xy} & \tau_{xz} \\ \tau_{yx} & \sigma_{yy} & \tau_{yz} \\ \tau_{zx} & \tau_{zy} & \sigma_{zz} \end{bmatrix}$$

5

Stress-Controlled Instability Mechanisms

Kaiser et al. (2000)

Stress-Controlled Instability Mechanisms

Although the fundamental complexity of the nature of stress has to be fully considered in the design of an underground excavation, the problem can be initially simplified through the assumptions of continuous, homogeneous, isotropic, linear elastic behaviour (CHILE).

CHILE: Continuous, Homogeneous, Isotropic, Linear Elastic

DIANE: Discontinuous, Inhomogeneous, Anisotropic, Non-Elastic

The engineering question is whether a solution based on the CHILE assumption are of any assistance in design. In fact though, many CHILE-based solutions have been used successfully, especially in those excavations at depth where high stresses have closed the fractures and the rock mass is relatively homogeneous and isotropic. However, in near-surface excavations, where the rock stresses are lower, the fractures more frequent, and the rock mass more disturbed and weathered, there is more concern about the validity of the CHILE model.

Stress-Controlled Instability Mechanisms

A stress analysis begins with a knowledge of the **magnitudes** and **directions** of the *in situ stresses* in the region of the excavation. This allows for the calculation of the excavation disturbed or **induced** stresses.

Brady & Brown (2006)
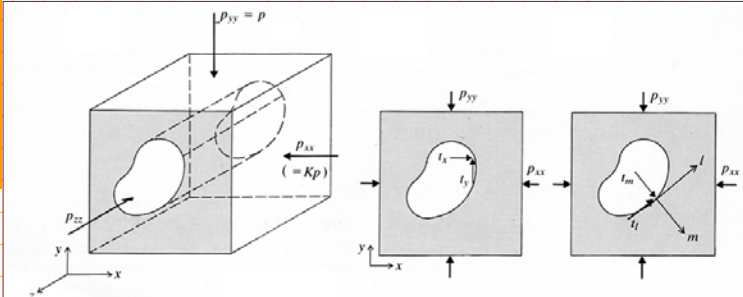
There exists several **close form solutions** for the induced stresses around circular and elliptical openings (and complex variable techniques extend these to many smooth, symmetrical geometries), and with **numerical analysis techniques** the values of the induced stresses can be determined accurately for any three-dimensional excavation geometry.

Stresses & Displacements – Circular Excavations

The **Kirsch equations** are a set of closed-form solutions, derived from the theory of **elasticity**, used to calculate the stresses and displacements around a **circular excavation**.
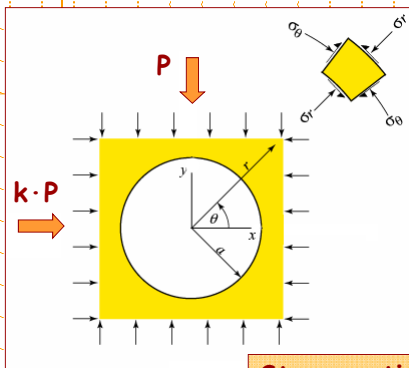
$$\sigma_{rr} = \frac{p}{2}\left[(1+K)\left(1-\frac{a^2}{r^2}\right)-(1-K)\left(1-4\frac{a^2}{r^2}+\frac{3a^4}{r^4}\right)\cos 2\theta\right]$$

$$\sigma_{\theta\theta} = \frac{p}{2}\left[(1+K)\left(1+\frac{a^2}{r^2}\right)+(1-K)\left(1+\frac{3a^4}{r^4}\right)\cos 2\theta\right]$$

$$\sigma_{r\theta} = \frac{p}{2}\left[(1-K)\left(1+\frac{2a^2}{r^2}-\frac{3a^4}{r^4}\right)\sin 2\theta\right]$$

$$u_r = -\frac{pa^2}{4Gr}\left[(1+K)-(1-K)\left\{4(1-v)-\frac{a^2}{r^2}\right\}\cos 2\theta\right]$$

$$u_\theta = -\frac{pa^2}{4Gr}\left[(1-K)\left\{2(1-2v)+\frac{a^2}{r^2}\right\}\sin 2\theta\right]$$

Brady & Brown (2006)

Stress ratio:

$k = \sigma_h/\sigma_v$

Stresses & Displacements - Circular Excavations

From these equations we can see that the stresses on the boundary (i.e. when r = a) are given by:

$$\sigma_{\theta\theta} = p[(1+k) + 2(1-k)\cos 2\theta]$$

$$\sigma_{rr} = 0$$

$$\tau_{r\theta} = 0$$

Note that the radial stresses are zero because there is no internal pressure, and the shear stresses must be zero at a traction-free boundary.
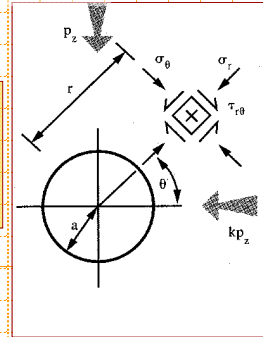
Example #1: Stresses around a Circular Opening

Q. At a depth of 750 m, a 10-m diameter circular tunnel is driven in rock having a unit weight of 26 kN/m³ and uniaxial compressive and tensile strengths of 80.0 MPa and 3.0 MPa, respectively. Will the strength of the rock on the tunnel boundary be exceeded if:

    (a) k=0.3,   (b) k=2.0?
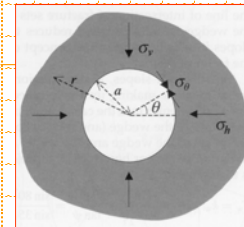
Harrison & Hudson (2000)

A. Since the tunnel has neither a support pressure nor an internal pressure applied to it, the local stresses at the boundary have $\sigma_3 = \sigma_r = 0$ and $\sigma_1 = \sigma_\theta$. The Kirsch solution for the circumferential stress is:

$$\sigma_\theta = \tfrac{1}{2}\sigma_v \left[(1+k)\left(1 + \frac{a^2}{r^2}\right) + (1-k)\left(1 + 3\frac{a^4}{r^4}\right)\cos 2\theta \right]$$

For a location on the tunnel boundary (i.e. a = r), this simplifies to:

$$\sigma_\theta = \sigma_v \left[(1+k) + 2(1-k)\cos 2\theta\right]$$

8

Example #1: Stresses around a Circular Opening

Q. Circular tunnel: 750 m deep, 10m diameter, γ_{rock} = 26 kN/m³, σ_{UCS} = 80.0 MPa, σ_T = 3.0 MPa. Will the strength of the rock on the tunnel boundary be reached if: (a) k=0.3, and (b) k=2.0?
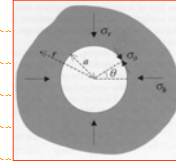
A. We assume that the vertical stress is caused by the weight of the overburden, in which case we have:

$$\sigma_v \ = \ \gamma\,z \ = \ 0.026 \times 750 \ = \ 19.5\ MPa$$

The extreme values of induced stress occur at positions aligned with the principal *in situ* stresses, and so in order to compute the stress induced in the crown and invert (i.e. roof and floor) we use θ = 90°, and for the sidewalls we use θ = 0°.

Example #1: Stresses around a Circular Opening

Q. Circular tunnel: 750 m deep, 10m diameter, γ_{rock} = 26 kN/m³, σ_{UCS} = 80.0 MPa, σ_T = 3.0 MPa. Will the strength of the rock on the tunnel boundary be reached if: (a) k=0.3, and (b) k=2.0?
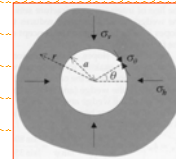
A. For k=0.3:

Crown and invert (θ = 90°), σ_θ = –1.95 MPa (i.e. tensile)
Sidewalls (θ = 0°), σ_θ = 52.7 MPa

For k=2.0:

Crown and invert (θ = 90°), σ_θ = 97.5 MPa
Sidewalls (θ = 0°), σ_θ = 19.5 MPa

compressive strength is exceeded

9

Stress and Failure Criterion
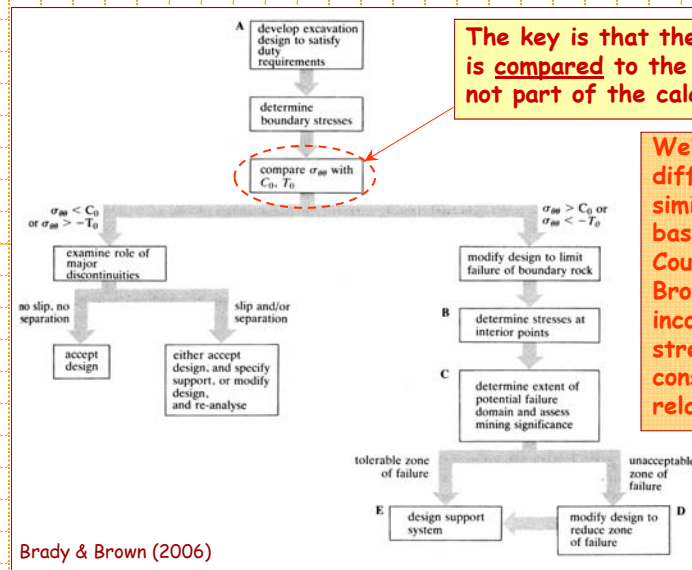
The key is that the failure criterion is **compared** to the stresses and is not part of the calculation!!

We'll see this is different when similar relationships based on Mohr-Coulomb and Hoek-Brown are incorporated into stress-strain constitutive relationships.

Brady & Brown (2006)

Orientation of σ_1 & Induced Stresses
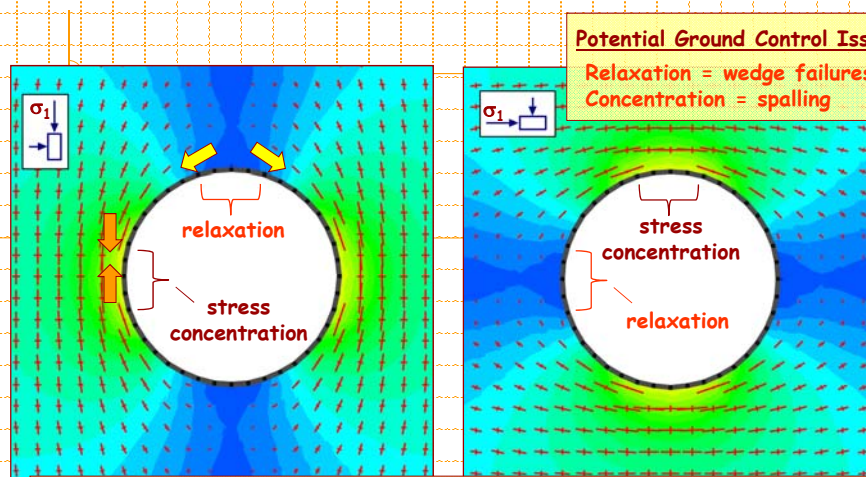
Potential Ground Control Issues:
Relaxation = wedge failures
Concentration = spalling

σ_1

relaxation

stress concentration

σ_1

stress concentration

relaxation

Stresses can be visualized as flowing around the excavation periphery in the direction of the major principle stress (σ_1). Where they diverge, relaxation occurs; where they converge, stress increases occur.

10

Conservation of Load

Another concept that can be elegantly demonstrated from the Kirsch equations is the principle of conservation of load.

... principle of conservation of load before and after excavation. The sketches show how the distribution of vertical stresses across a horizontal plane changes.
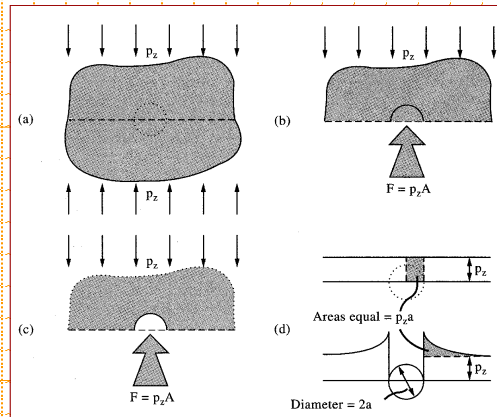
Hudson & Harrison (1997)

Stresses Away from Opening
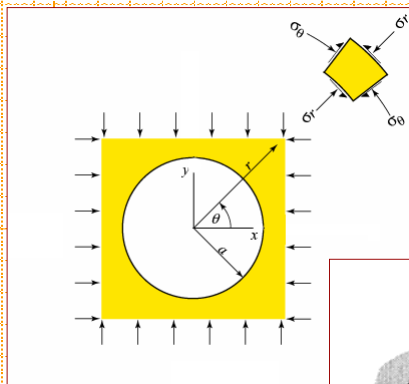
$$\sigma_r = \tfrac{1}{2}p_z \left\{ (1+k)\left(1 - \frac{a^2}{r^2}\right) - (1-k)\left(1 - 4\frac{a^2}{r^2} + 3\frac{a^4}{r^4}\right)\cos 2\theta \right\}$$

$$\sigma_\theta = \tfrac{1}{2}p_z \left\{ (1+k)\left(1 + \frac{a^2}{r^2}\right) + (1-k)\left(1 + 3\frac{a^4}{r^4}\right)\cos 2\theta \right\}$$

$$\tau_{r\theta} = \tfrac{1}{2}p_z \left\{ (1-k)\left(1 + 2\frac{a^2}{r^2} - 3\frac{a^4}{r^4}\right)\sin 2\theta \right\}$$

11
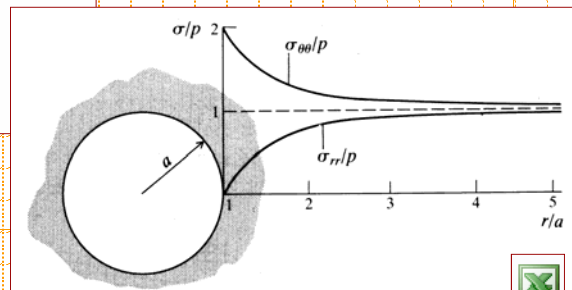
Zone of Influence

The concept of influence is important in excavation design, since the presence of a neighbouring opening may provide a significant disturbance to the near-field stresses to the point of causing failure.

… (a) axisymmetric stress distribution around a circular opening in a hydrostatic stress field; (b) circular openings in a hydrostatic stress field, effectively isolated by virtue of their exclusion from each other's zone of influence.
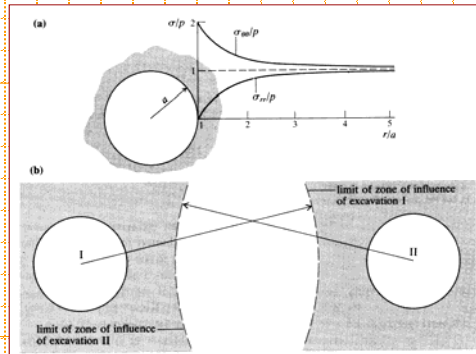
Brady & Brown (2006)
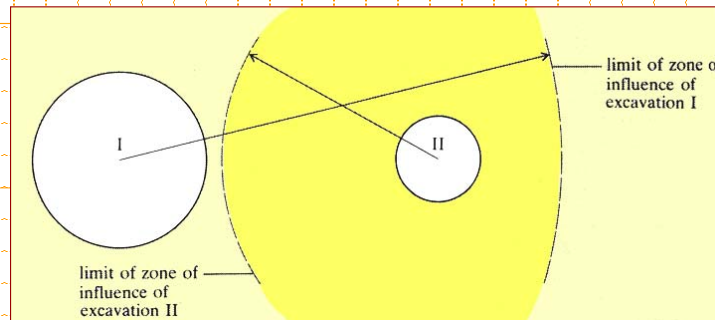
Zone of Influence

Brady & Brown (2006)

… illustration of the effect of contiguous openings of different dimensions. The zone of influence of excavation I includes excavation II, but the converse does not apply.

12

Stresses Around Elliptical Openings
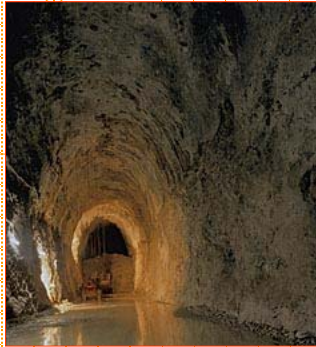
The stresses around elliptical openings can be treated in an analogous way to that just presented for circular openings. There is much greater utility associated with the solution for elliptical openings than circular openings, because these can provide a first approximation to a wide range of engineering geometries, especially openings with high width/height ratios (e.g. mine stopes, power house caverns, etc.).

From a design point of view, the effects of changing either the orientation within the stress field or the aspect ratio of such elliptical openings can be studied to optimize stability.

Stresses Around Elliptical Openings

Assuming isotropic rock conditions, an elliptical opening is completely characterized by two parameters: aspect ratio (major to minor axis) which is the eccentricity of the ellipse; and orientation with respect to the principle stresses. The position on the boundary, with reference to the x-axis, is given by the angle χ.
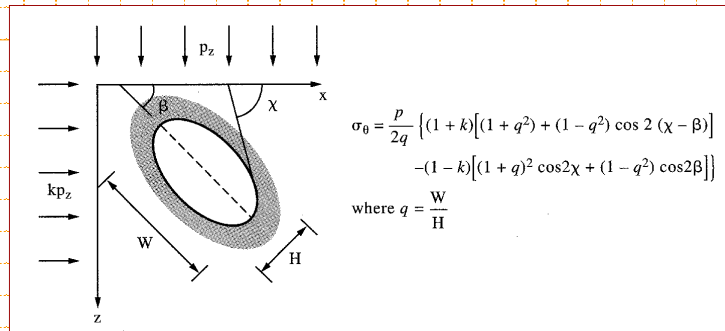
$$\sigma_\theta = \frac{p}{2q}\left\{(1+k)\left[(1+q^2)+(1-q^2)\cos 2\,(\chi-\beta)\right]\right.$$
$$\left.-(1-k)\left[(1+q)^2\cos 2\chi + (1-q^2)\cos 2\beta\right]\right\}$$
$$\text{where } q = \frac{W}{H}$$

Hudson & Harrison (1997)

13

Stresses Around Elliptical Openings

It is instructive to consider the **maximum** and **minimum** values of the **stress concentrations** around the ellipse for the geometry of an ellipse aligned with the principal stresses. It can be easily established that the extremes of stress concentration occur at the ends of the major and minor axes.

$$\sigma_A = p(1 - k + 2q) = p\left(1 - k + \sqrt{\frac{2W}{\rho_A}}\right),$$

$$\sigma_B = p\left(k - 1 + \frac{2k}{q}\right) = p\left(k - 1 + k\sqrt{\frac{2H}{\rho_B}}\right)$$

where, for an ellipse, the radii of curvature are

$$\rho_A = \frac{H^2}{2W} \quad \text{and} \quad \rho_B = \frac{W^2}{2H}$$

Hudson & Harrison (1997)

Example #2: Stresses around an Elliptical Opening

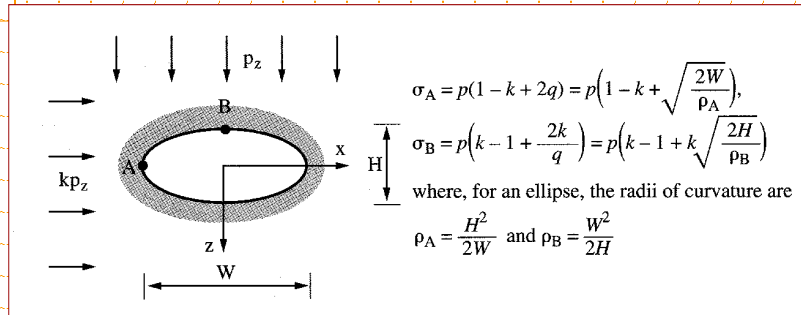**Q.** A gold-bearing quartz vein, 2 m thick and dipping 90°, is to be exploited by a small cut-and-fill stoping operation. The mining is to take place at a depth of 800 m, and the average unit weight of the granite host rock above this level is 29 kN/m3. The strike of the vein is parallel to the intermediate stress, and the major principal stress is horizontal with a magnitude of 37.0 MPa. The uniaxial compressive strength of the vein material is 218 MPa, and the tensile strength of the host rock is –5 MPa. What is the maximum permissible stope height before failure occurs.

A. We can assume that, in 2-D cross-section, the stresses induced in the sidewalls (tensile) and the crown (compressive) of the stope can be approximated using the equations for an elliptical excavation.

$$\frac{\sigma_{\text{sidewall}}}{\sigma_{\text{vertical}}} = 1 - k + 2\left(\frac{w}{h}\right)$$

$$\frac{\sigma_{\text{crown}}}{\sigma_{\text{vertical}}} = k - 1 + k\sqrt{\frac{2h}{\rho_{\text{crown}}}} = k - 1 + 2k\sqrt{\frac{h}{w}}.$$
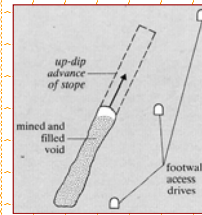
14

Example #2: Stresses around an Elliptical Opening

Q. Gold-bearing quartz vein: 2 m thick, dipping 90°. The mining stope is 800 m deep, γ = 29 kN/m3, strike parallel to σ_2, σ_1 = 37.0 MPa and is horizontal, $\sigma_{UCS\ (vein)}$ = 218 MPa, $T_{o\ (host\ rock)}$ = -5 MPa. What is the maximum permissible stope height before failure occurs.

A. Rearranging the given equations, we can solve for the height of the excavation as the minimum of:

$$h = \frac{2w}{\dfrac{\sigma_{\text{sidewall}}}{\sigma_{\text{vertical}}} + k - 1} \quad \textbf{or} \quad h = \frac{w}{4k^2}\left(\frac{\sigma_{\text{crown}}}{\sigma_{\text{vertical}}} + 1 - k\right)^2$$

The maximum stress that can be sustained by the crown and the sidewall are 218 and –5 MPa, respectively. Note that the sidewall stress is negative because this represents the tensile strength.
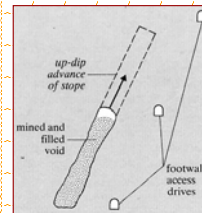

Example #2: Stresses around an Elliptical Opening

Q. Gold-bearing quartz vein: 2 m thick, dipping 90°. The mining stope is 800 m deep, γ = 29 kN/m3, strike parallel to σ_2, σ_1 = 37.0 MPa and is horizontal, $\sigma_{UCS\ (vein)}$ = 218 MPa, $T_{o\ (host\ rock)}$ = -5 MPa. What is the maximum permissible stope height before failure occurs.

A. The vertical stress is:

$$\sigma_{\text{vertical}} = \gamma \cdot z = 0.029 \times 800 = 23.2 \text{ MPa}$$

and hence the ratio of horizontal to vertical stress is:
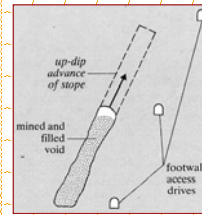
$$k = \frac{37.0}{23.2} = 1.59.$$

Example #2: Stresses around an Elliptical Opening

Q. Gold-bearing quartz vein: 2 m thick, dipping 90°. The mining stope is 800 m deep, γ = 29 kN/m3, strike parallel to σ_2, σ_1 = 37.0 MPa and is horizontal, $\sigma_{UCS\ (vein)}$ = 218 MPa, $T_{o\ (host\ rock)}$ = -5 MPa. What is the maximum permissible stope height before failure occurs.

A. The maximal height of a stope such that the compressive strength of the rock in the crown is not exceeded is given by:

$$h = \frac{w}{4k^2}\left(\frac{\sigma_{crown}}{\sigma_{vertical}} + 1 - k\right)^2 = \frac{2}{4 \times 1.59^2}\left(\frac{218}{23.2} + 1 - 1.59\right)^2 = 15.3 \text{ m.}$$

The maximal height of a stope such that the tensile strength of the rock in the sidewall is not exceeded is given by:

$$h = \frac{2w}{\dfrac{\sigma_{sidewall}}{\sigma_{vertical}} + k - 1} = \frac{2 \times 2}{\dfrac{-5}{23.2} + 1.59 - 1} = 10.7 \text{ m.}$$

Thus we see that sidewall failure is the limiting condition in the stope design.

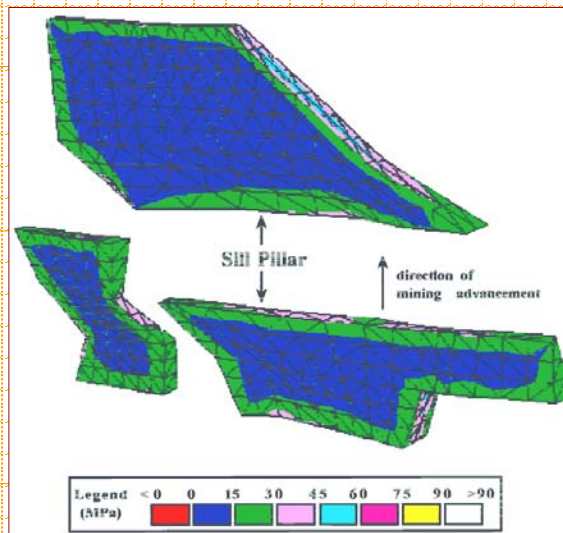## Stress Analysis – Numerical Modelling

Many underground excavations are **irregular** in shape and are frequently grouped close to **other excavations**. These problems require the use of **numerical techniques**.
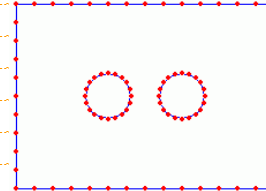

Eberhardt *et al.* (1997)

16

Numerical Modelling

Numerical methods of stress and deformation analysis fall into two categories:

**Integral Methods**

- incl. boundary-element method
- only problem boundary is defined & discretized
- <u>Pro</u>: more computationally efficient
  <u>Con</u>: restricted to elastic analyses

Differential Methods

- incl. finite-element/-difference & distinct-element methods
- problem domain is defined & discretized
- <u>Pro</u>: non-linear & heterogeneous material properties accommodated
 <u>Con</u>: longer solution run times
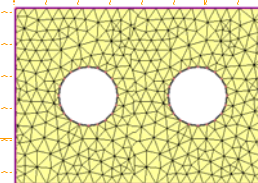
---

Boundary-Element & Stress Analyses

The Boundary Element Method (BEM) is generally favoured for stress analyses involving multiple excavations with complex 3-D geometries (e.g. those frequently encountered in underground mine design). The irregular shape of the orebodies and staged nature of mining, makes the ease of mesh generation and computational efficiency afforded by the BEM highly advantageous.
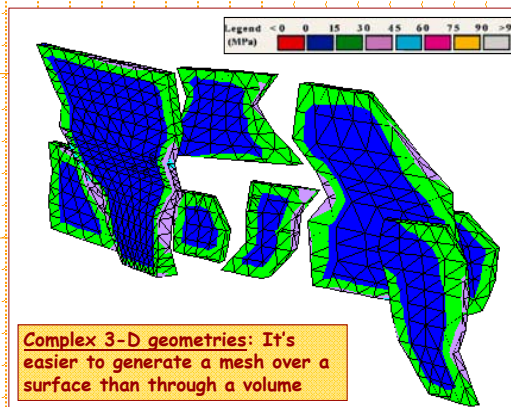
<u>Complex 3-D geometries</u>: It's easier to generate a mesh over a surface than through a volume

Eberhardt *et al.* (1997)

<u>Commercial Software:</u>

Examine3D (Rocscience) - http://www.rocscience.com/
Map3D (Mine Modelling Pty Ltd.) - http://www.map3d.com/
BEFE (Computer Software & Services - CSS) - http://members.chello.at/sylvia.beer/
GPBEST (Best Corp.) - http://www.gpbest.com/
BEASY (Beasy Group) - http://www.beasy.com/

Boundary-Element & Stress Analyses

In performing an analysis, the boundary of the excavation is divided into elements and the interior of the rock mass is represented mathematically as an infinite continuum. The solution works to find a set of approximate stresses which satisfy prescribed boundary conditions, and then uses these to calculate the stresses and displacements in the rock mass.
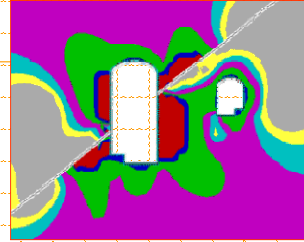
What to Know:

- Computational method of solving linear partial differential equations which have been formulated as integral equations (i.e. in boundary integral form).

- Key advantage is the reduction of the model dimension by one, providing simpler mesh generation & input data preparation, and greater computational efficiency.

- Key disadvantage is the required assumption of homogeneous linear elastic material behaviour; plasticity and heterogeneity negate the method's intrinsic simplicity.

- Common applications include stress analysis of underground excavations, soil-structure interactions, brittle fracturing processes, dynamic problems, groundwater flow and coupled H-M & T-H-M problems.
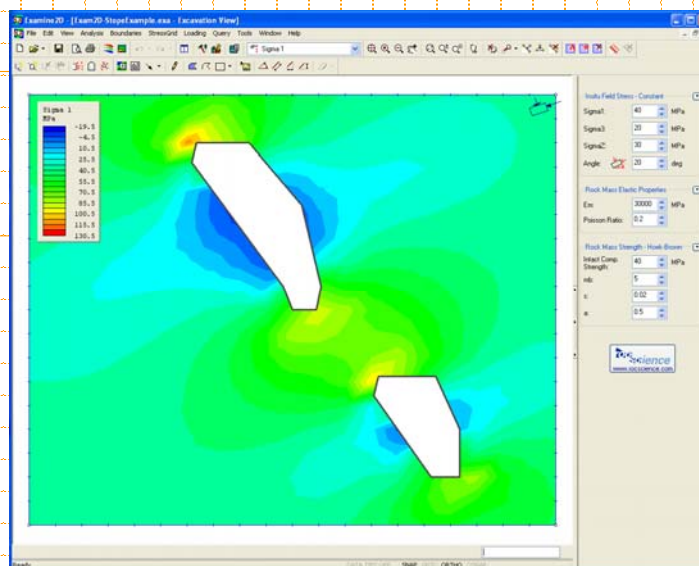

Boundary-Element & Stress Analysis

18

Stress Analysis & Failure

σ_1
failure
in situ stress
σ_3

p_1
p_2

p_1
p_2

4 m
2 m
6 m

Observed Failure

σ_{ci} = 100 MPa
m = 0
s = 0.11

1.8m
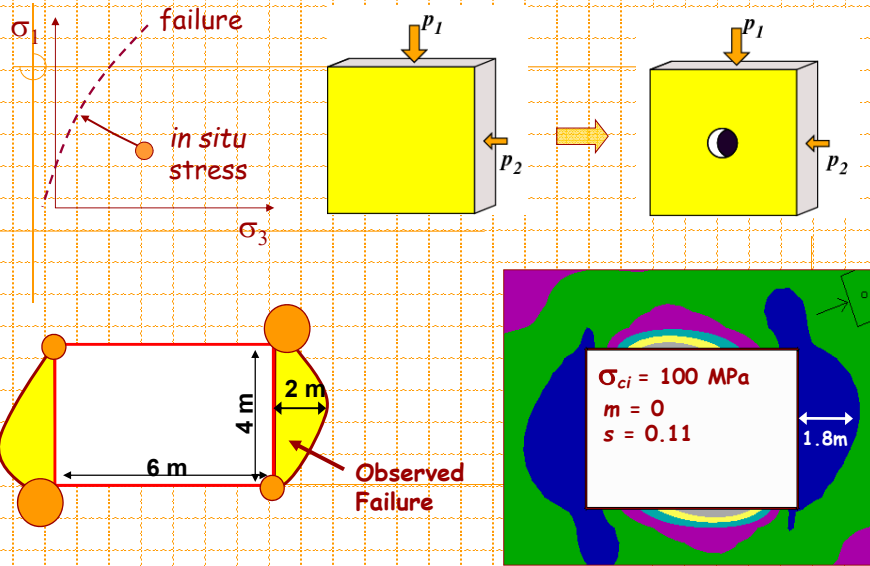
In-Situ Stresses – Canadian Shield

Stresses in the Canadian Shield typically involve high horizontal stresses that are twice the vertical stresses.

Method:
focal mechanism
breakouts
drill. induced frac.
borehole slotter
overcoring
hydro. fractures
geol. indicators
Regime:
NF SS TF U
Quality:
A
B
C
all depths
© (2008) World Stress Map

Heidbach et al. (2008)
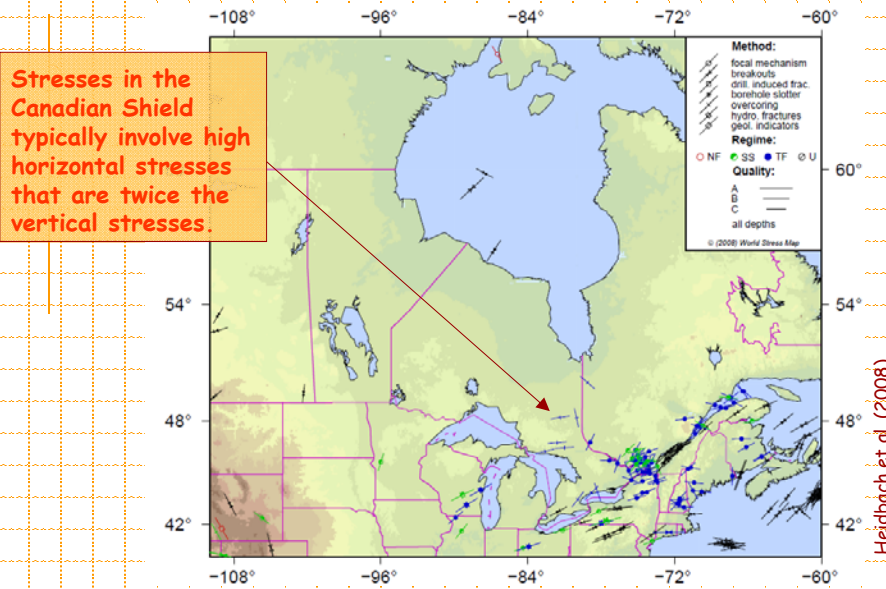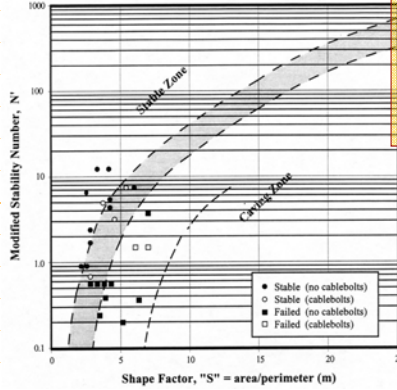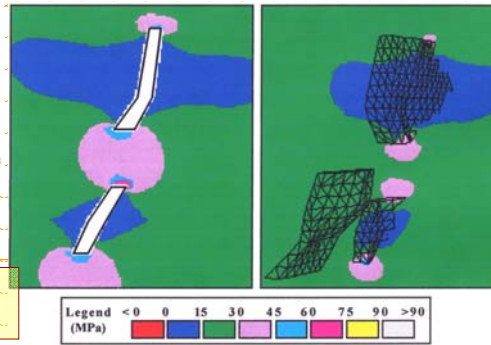
Case History: Trout Lake Mine Stress Analysis

Reschke & Romanowski (1993)

Empirical analysis based on performance of stope backs in the Flin Flon deposits, although useful, may be limited in its applicability if the database is populated with cases at shallower depths (i.e. lower stresses).

Eberhardt *et al.* (1997)
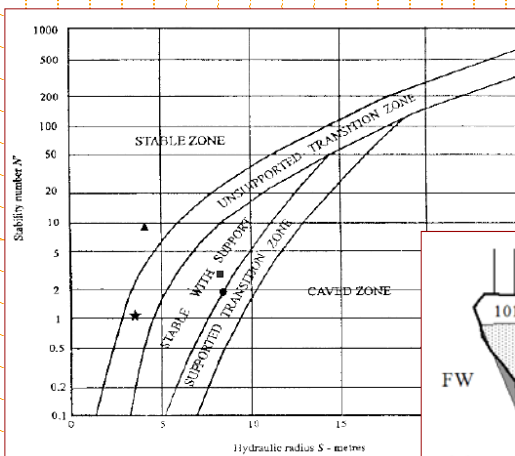
2-D and 3-D stress analyses of Trout Lake stopes.
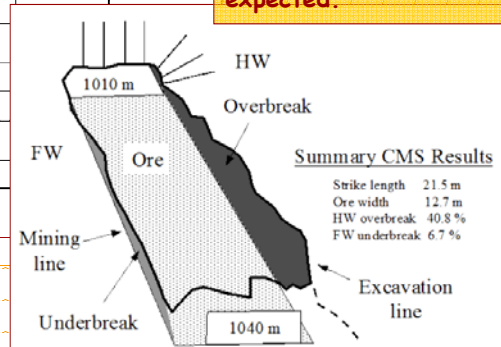
Test Stope at Depth

Stability charts indicate that stopes at 1000m depth will require cable bolting. Without it, significant hangingwall dilution (40%) would be expected.
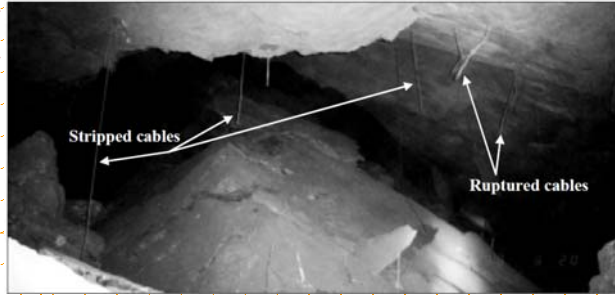
Summary CMS Results

Strike length	21.5 m
Ore width	12.7 m
HW overbreak	40.8 %
FW underbreak	6.7 %

deGraaf et al. (1993)

Test Stope at Depth

deGraaf et al. (1993)

Stripped cables

Ruptured cables

Smart cable monitoring of cablebolt loading in hangingwall .

Case History: Trout Lake Mine Stress Analysis

Eberhardt et al. (1997)
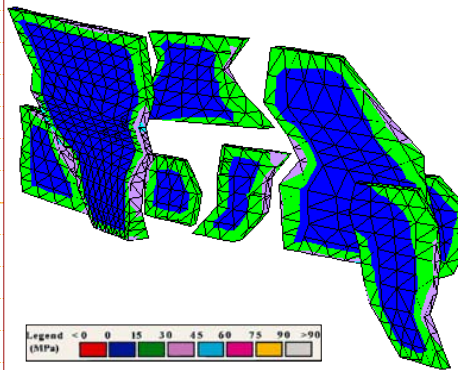
3-D boundary element analyses help to examine the stress interactions between neighbouring stopes.

Legend < 0 0 15 30 45 60 75 90 >90 (MPa)

Sill Pillar

direction of mining advancement
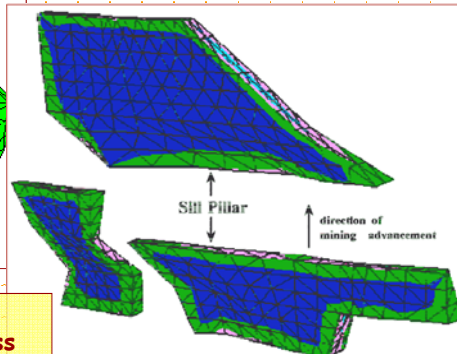
Computed stresses can then be compared against estimated rock mass strengths to assess pillar stability.

Legend < 0 0 15 30 45 60 75 90 >90 (MPa)

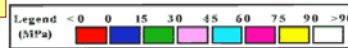## Sill Pillar Thickness

Elastic Sill Pillar Analysis

pillar

stope back

Legend (MPa) < 35 35 45 50 55 60 65 70 75 80 >85

yield zone

stope back

Sill Pillar

direction of mining advancement

Legend (MPa) <0 0 15 30 45 60 75 90 >90
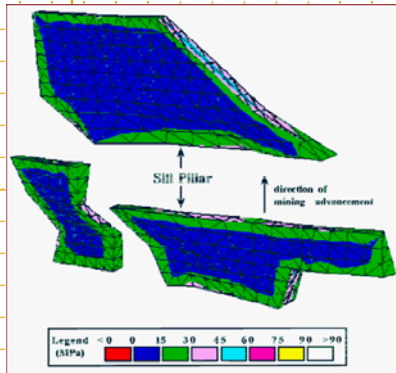
Eberhardt et al. (1997)
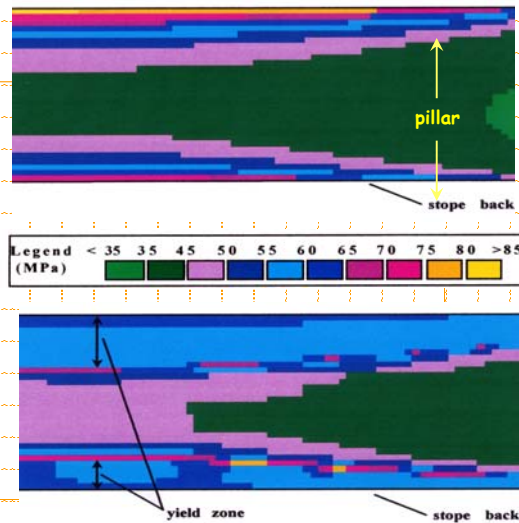
Elasto-Plastic Sill Pillar Analysis

Sill Pillar Value

Pillars represent either temporary or permanent sterilisation of a fully proven and developed ore reserve. Calculate the value of the Trout Lake sill pillar, using the spreadsheet provided and the following assumptions.

- Production grades: 2.18% Cu, 3.65% Zn, 1.28g/t Au, and 13.53g/t Ag.

- Operating costs: $42/tonne.

- Sill pillar footprint: 2000 m^2

Lecture References

Brady, BHG & Brown, ET (2006). Rock Mechanics for Underground Mining (3rd Edition). Chapman & Hall: London.

DeGraaf, PJH, Hyett, AJ, Lausch, P, Bawden, WF & Yao, M (1999). Hudson Bay Mining and Smelting Co.'s field trials using 'SMART' technology – successful ground support design through in situ cable bolt performance evaluation. In *Proceedings of the 101st Annual General Meeting of CIM, Calgary*.

Eberhardt, E, Stead, D, Reeves, MJ & Connors, C (1997). Design of tabular excavations in foliated rock: An integrated numerical modelling approach. *Geotechnical and Geological Engineering* **15** (1): 47-85.

Harrison, JP & Hudson, JA (2000). Engineering Rock Mechanics – Part 2: Illustrative Worked Examples. Elsevier Science: Oxford.

Heidbach, O, Tingay, M, Barth, A, Reinecker, J, Kurfeß, D & Müller, B (2008). The World Stress Map database release 2008. doi:10.1594/GFZ.WSM.Rel2008.

Hudson, JA & Harrison, JP (1997). Engineering Rock Mechanics – An Introduction to the Principles . Elsevier Science: Oxford.

Kaiser, PK, Diederichs, MS, Martin, D, Sharpe, J & Steiner, W (2000). Underground works in hard rock tunnelling and mining. In *GeoEng2000, Melbourne*. Technomic Publishing Company: Lancaster, pp. 841-926.

Reschke, AE & Romanowski, J (1993). The success and limitations of Mathews analysis for open stope design at HBMS, Flin Flon operations. In *95th CIM Annual General Meeting, Calgary*. Paper #136, 13 pp.

23